

[Interactive
Comment](#)

Interactive comment on “Observations of the scale-dependent turbulence and evaluation of the flux-gradient relationship for sensible heat for a closed Douglas-Fir canopy in very weak wind conditions” by D. Vickers and C. Thomas

D. Vickers and C. Thomas

vickers@coas.oregonstate.edu

Received and published: 1 July 2014

[12pt]article

epsfig graphics

[Full Screen / Esc](#)

[Printer-friendly Version](#)

[Interactive Discussion](#)

[Discussion Paper](#)



1 Response to reviewer 1

As suggested by the reviewer, there is large uncertainty in the night-time subcanopy momentum fluxes at the smallest resolved timescales. This is evident in the modified Figs 2 and 3 showing error bars denoting the 99% confidence limits about the mean for all quantities and all timescales.

The "relatively" large momentum fluxes observed inside the canopy at night at the smallest resolved timescales appear to "go away" during the day, when the flux is larger and is dominated by transport on timescales of about a minute. By comparison, at night the momentum flux is smaller and is only weakly dependent on the perturbation timescale. In the plots, the daytime flux at the smallest timescales "goes away" because it is small compared to the flux at larger timescales.

The night-time subcanopy momentum fluxes for timescales of 1000 s appear to be negative (see modified Fig 3 with error bars); however, motions on the largest timescales are subject to the greatest uncertainty because they are the most poorly sampled. It is not clear if these fluxes are meaningful, or why the downward momentum transfer would tend to be largest at these longer timescales of order 15 minutes. Transfer on timescales this large may be associated with non-turbulent motions.

Regression of the 38-m heat flux on U_{38m} ($TS_{2cm}-Ta_{38m}$) gives an r-squared value of 0.52.

Yes, it would be very interesting to contrast the Stanton number for different forest canopies.

We removed all reference to gas analyzers.

We think the x-axis labels for Fig 7, 9 and 11 are clear as written.

We include all figures below.

Full Screen / Esc

Printer-friendly Version

Interactive Discussion

Discussion Paper



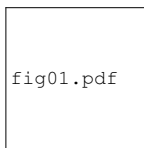


Fig. 1. The frequency distribution of the subcanopy mean wind speed (top) and the standard deviation of vertical velocity (bottom).



Fig. 2. Composites of three levels of daytime vertical velocity spectra ww ($\text{m}^2 \text{s}^{-2}$, left column), kinematic heat flux cospectra wT ($^{\circ}\text{C m s}^{-1}$, middle column), and the along- and cross-wind (red) components of the momentum flux (wu and wv) ($\text{m}^2 \text{s}^{-2}$, right column). All quantities have been multiplied by one-thousand. The error bars denote the 99% confidence limit about the mean. The vertical line in each panel denotes $\tau = 20$ s.



Fig. 3. Same as Figure 2 except for nighttime.

[Full Screen / Esc](#)[Printer-friendly Version](#)[Interactive Discussion](#)[Discussion Paper](#)

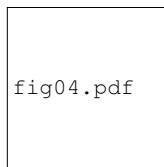


Fig. 4. Three levels of the scale-dependence of the velocity aspect ratio VAR. The vertical line denotes $\tau = 20$ s.

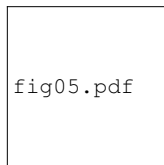


Fig. 5. The normalized turbulence intensity at three levels as a function of the wind speed above the canopy. Error bars denote \pm one standard error.



Fig. 6. The observed diurnal cycle of the subcanopy sensible heat flux with standard error bars (top) and \pm one standard deviation (bottom), where the uncertainty is due to the day-to-day variability in the heat flux for a given hour of the day over the entire 5-month period.

[Full Screen / Esc](#)[Printer-friendly Version](#)[Interactive Discussion](#)[Discussion Paper](#)

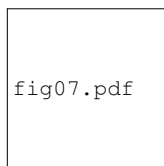


Fig. 7. Scatter plot of the 30-minute average subcanopy kinematic heat flux (lower panel) as a function of the product of the mean wind speed and the temperature difference. The slope of the linear regression line (red) is an estimate of the subcanopy Stanton number (C_H). The estimate for the subcanopy C_H using this approach is $1.1 \pm 0.04 \times 10^{-3}$, using a 90% confidence interval for the slope, and the regression explains 32% of the variance. Above the canopy at 38 m (upper panel), the estimate of the Stanton number is $73.5 \pm 1.3 \times 10^{-3}$, with 77% of the variance explained.



Fig. 8. The frequency distribution of the subcanopy Stanton number (multiplied by one-thousand) where each 30-minute estimate is computed as the heat flux divided by the product of the mean wind speed and the temperature difference. This approach for estimating the Stanton number yields a mean value of 1.1×10^{-3} and a standard deviation of 2.05×10^{-3} .

[Full Screen / Esc](#)[Printer-friendly Version](#)[Interactive Discussion](#)[Discussion Paper](#)

fig09.pdf

Fig. 9. The kinematic heat flux as a function of the product of the mean wind speed and the temperature difference at 38 m (top panel) and at 4 m (bottom). The slopes of the linear regression lines (red) are estimates of the Stanton number: $73.5 \pm 1.3 \times 10^{-3}$ at 38 m, and $1.1 \pm 0.04 \times 10^{-3}$ at 4 m. Each of the ten class averages contains an equal number (282) of 30-minute samples. Error bars denote \pm one standard error.


fig10.pdf

Fig. 10. The frequency distribution (top panel) and the diurnal cycle (bottom) of the above canopy Stanton number multiplied by one-thousand. Error bars denote \pm one standard error.

fig11.pdf

Fig. 11. The kinematic heat flux as a function of the product of the mean wind speed and the temperature difference using the single source approach (see text). The slope of the linear regression line (red) is estimate of the Stanton number: $-12.8 \pm 27.9 \times 10^{-3}$. Each of the ten class averages contains an equal number (282) of 30-minute samples. Error bars denote \pm one standard error.

[Full Screen / Esc](#)[Printer-friendly Version](#)[Interactive Discussion](#)[Discussion Paper](#)